Discrete-time mode switching control with application to a PMSM position servo system

Guoyang Cheng [a,*], Kemao Peng [b], Ben M. Chen [c], Tong H. Lee [c]

[a] College of Electrical Engineering and Automation, Fuzhou University, Fujian 350108, PR China
[b] The Temasek Laboratories, National University of Singapore, Singapore 117508, Singapore
[c] Department of Electrical and Computer Engineering, National University of Singapore, Singapore 117576, Singapore

ABSTRACT

This paper presents a mode switching control (MSC) scheme in discrete-time domain for fast and precise set-point tracking in servo systems subject to control saturation and unknown disturbance. The basic idea is to combine the proximate time-optimal servomechanism (PTOS) and the composite nonlinear feedback (CNF) control, using the output position as the only measurable information for feedback. The PTOS is responsible for fast targeting in servo systems when the tracking error is large, and once the system trajectory enters into some specified region, the CNF will take over the control to ensure a smooth settling without compromising the fast transient performance. A reduced-order extended state observer is adopted to estimate the speed signal for feedback and the disturbance for compensation. The asymptotical stability of the proposed MSC scheme is analyzed and the switching conditions are provided. Simulation and experimental results on a permanent magnet synchronous motor (PMSM) servo system verify that the proposed control scheme is effective in improving the tracking performance for a wide range of target set-points.

© 2013 Elsevier Ltd. All rights reserved.

1. Introduction

Rapid motion is required in a wide range of industrial production and assembly lines, for which control technology can play a vital role. In the context of point-to-point motion, two stages are usually involved. The first stage is fast targeting, which drives the system output from the present position into the neighborhood of a specified destination in minimum time using a bounded control effort. Next comes the second stage, i.e., smooth settling, which maintains the system output as close as possible to the destination position, in the face of power limitation, various disturbances and uncertainties in real application environment. Due to the different specifications for targeting and settling modes, it is quite difficult to design a controller that can achieve excellent performance in both modes using one single control technology. Usually, different control techniques will be used to design control laws for fast targeting and smooth settling respectively, and then some switching strategy is adopted to ensure the successful transition. This is the principle of mode switching control (MSC).

For double-integrator systems, Workman [1] proposed the proximate time-optimal servomechanisms (PTOS) (see also [2]), which switches smoothly from the time optimal control (TOC)

law to a linear control law when the tracking error is small, thus avoids the chattering problem of TOC and enhances the robustness, at the cost of some degradation in transient performance. In essence, the PTOS is some kind of MSC scheme, which can be easily implemented and obtain almost optimal performance in tracking a large stroke target. Hence, the PTOS emerges as a desirable solution for fast targeting. However, when it comes to smooth settling, there is scope for improvements on the linear part of PTOS. As is well known, linear control laws always have to make a trade-off between fast response and low overshoot, for the given closed-loop bandwidth. During the past decade, there had been some research efforts to improve PTOS. For example, Zhou et al. [3] combined the PTOS with sliding-mode control and achieved smooth mode transition and better performance. Choi et al. [4] proposed a modified PTOS scheme with a gain-scheduled damping which resulted in faster settling. Both [3,4] assumed that the state variables are available for feedback control. Venkataramanan et al. [5] developed an MSC scheme with measurement feedback in continuous-time domain by combining the PTOS with a robust perfect tracking (RPT) control law. But the RPT suffers the same limitation of linear control, notwithstanding its robustness against external disturbances and initial values. Moreover, the problem of disturbance compensation was not considered.

In this paper, a composite nonlinear feedback (CNF) control law is incorporated into the PTOS framework to develop an MSC control scheme in discrete-time domain. The CNF control law consists

* Corresponding author. Tel.: +86 13559127925.
E-mail addresses: cheng@fzu.edu.cn (G. Cheng), kmpeng@nus.edu.sg (K. Peng), bmchen@nus.edu.sg (B.M. Chen), eleleeth@nus.edu.sg (T.H. Lee).

of a linear feedback part for yielding a fast response, and a nonlinear feedback part to tune the closed-loop damping-ratio to smooth out the overshoot (see [6,7]). By enforcing a dynamic closed-loop damping ratio (from lightly damped to heavily damped), the CNF control system can achieve fast and smooth transient performance in set-point tracking tasks, and has been successfully implemented in HDD servo system test-beds (see e.g., [7–10]) and unmanned helicopter (see e.g., [11,12]). However, the operation range, or the maximum amplitude of target reference of a CNF control system is limited by its invariant set, which in turn depends on the design parameters. To maintain the good transient performance, the parameters of CNF may have to be re-tuned for different target references. In [13], a unified control scheme (UCS) was proposed for track seeking and following in disk drive servo system. This control scheme is essentially some kind of multi-stage MSC. However, the operation of UCS is still limited to short-span tracking, once its design is fixed. In the MSC scheme proposed here, the PTOS control law is initially used for large stroke tracking, and as the tracking error gets smaller, the system state falls into some defined region, then the CNF control will take over to ensure a fast and smooth settling. An extended state observer is adopted to estimate the speed signal for feedback and the disturbance for compensation. With the proposed MSC, there is no limitation on the operation range, for the given input saturation level. Moreover, we would like to note that, in real applications, a controller designed in continuous-time domain eventually has to be discretized for digital implementation. Hence it seems more meaningful to design controllers directly in the discrete-time domain whenever possible. Further, it turned out that the stability analysis in our discrete-time MSC is quite different from that in the continuous case.

This paper is organized as follows. A discrete-time MSC control method which combines PTOS and CNF control is presented in Section 2. In Section 3, we apply the MSC control methodology to design a controller for a permanent magnet synchronous motor (PMSM) servo system. Simulation and experimental results are provided. Finally, we draw some concluding remarks in Section 4.

2. Discrete-time mode switching control

In this section, we present a discrete-time MSC control method for typical servo systems characterized by a double-integrator, of which a discretized state-space model can be formulated as follows:

$$x(k + 1) = A \cdot x(k) + B \cdot [\text{sat}(u(k)) + d], \quad (1)$$

with

$$x(k) = \begin{pmatrix} y(k) \\ v(k) \end{pmatrix}, \quad A = \begin{bmatrix} 1 & T \\ 0 & 1 \end{bmatrix}, \quad B = \begin{bmatrix} \frac{1}{2}aT^2 \\ aT \end{bmatrix}.$$

where $x(k) \in \mathbb{R}^2$ and $u(k)$ are the state and control variables respectively of the plant. $y(k)$ is the only measurable output (position) and $v(k)$ represents the velocity signal. d is the unknown constant or slowly-varying disturbance. T is the sampling period, a is the acceleration constant and assumed to be positive for simplicity. $\text{sat} : \mathbb{R} \to \mathbb{R}$ represents the actuator saturation defined as

$$\text{sat}(u(k)) = \text{sgn}(u(k)) \cdot \min\{u_{\max}, |u(k)|\}, \quad (2)$$

with $u_{\max}$ being the saturation level, and $\text{sgn}(\cdot)$ represents the sign function. The plant (1) can be reformulated as follows,

$$\begin{pmatrix} e(k + 1) \\ v(k + 1) \end{pmatrix} = \begin{bmatrix} 1 & -T \\ 0 & 1 \end{bmatrix} \begin{pmatrix} e(k) \\ v(k) \end{pmatrix} + \begin{bmatrix} -\frac{1}{2}aT^2 \\ aT \end{bmatrix} [\text{sat}(u(k)) + d], \quad (3)$$

where $e(k) = r - y(k)$ is the tracking error, and r is the target reference.

The MSC is a special type of variable structure control systems with the switching action occurring in a unidirectional way. Fig. 1 is a schematic diagram of the proposed MSC control. There are two servo modes for tracking tasks. Each mode can be designed independently. The critical issue in MSC control is the design of a switching mechanism, which is still a headache to date, although there have been a lot of research efforts on it. In the proposed MSC scheme, the PTOS control law is effective in the region of large tracking error because it can diminish the large tracking error in a near minimal time, almost same as the time optimal control does [1]. The CNF control law is applied to the small tracking error to achieve fast and smooth settling. In the following three subsections, we will present the MSC control scheme in details together with stability analysis. Mode switching conditions will also be discussed.

2.1. Discrete-time observer-based robust PTOS control

In this section, we will present the discrete-time robust PTOS control with measurement feedback for the plant (1). The discrete-time PTOS control law, originally proposed by Workman [1] and lately modified in [2], is based on state feedback and can be given by

$$u_P(k) = \text{sat}(k_2[f(e(k)) - v(k)]), \quad (4)$$

$$f(e(k)) = \begin{cases} \frac{k_1}{k_2} e(k), & |e(k)| \leqslant y_l, \\ \text{sgn}(e(k))[\sqrt{2au_{\max}\alpha|e(k)|} - J_0], & |e(k)| > y_l, \end{cases} \quad (5)$$

where k_1 and k_2 are respectively the feedback gains for position and velocity, $\alpha \in (0, 1)$ is a constant referred to as the acceleration discount factor, y_l is the size of the linear region, and J_0 is an offset for velocity signal. The feedback gains k_1 and k_2 can be designed by using pole placement for a conjugate pair of poles with the damping ratio ζ and natural frequency ω as two independent design parameters,

$$k_1 = \frac{p_1 + p_0 + 1}{aT^2}, k_2 = \frac{p_1 - p_0 + 3}{2aT}. \quad (6)$$

where

$$p_1 = -2e^{-\zeta\omega T} \cos(\omega T\sqrt{1 - \zeta^2}), p_0 = e^{-2\zeta\omega T}.$$

Further more,

$$J_0 = \frac{a\alpha u_{\max}T}{4} \left(\frac{p_1 - p_0 + 3}{p_1 + p_0 + 1}\right), \quad y_l = \frac{2J_0^2}{a\alpha u_{\max}}. \quad (7)$$

It was proved by Workman in [1] that the closed-loop system comprising the discrete-time PTOS control law with state feedback (4) and the plant (3) without disturbance is asymptotically stable provided that the following conditions are satisfied.
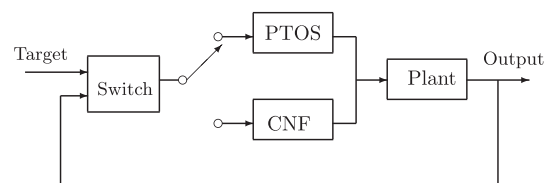
Conditions:

1. $aTk_2 \in (0, 2)$;

Fig. 1. Schematic diagram of MSC control.

2. $f(0) = 0$;

3. $f(e)e > 0$, for $\forall e \neq 0$;

4. $\lim_{e \to \infty} \int_0^e f(\sigma)d\sigma = \infty$;

5. $\dot{f}(e)$ exists for $\forall e$;

6. $|\dot{f}(e)| < \frac{2}{T}$ for $\forall e$; and

7. $|f(e + \Delta e) - (v + \Delta v)| < \frac{u_{\max}}{k_2}$ for $\forall(e, v)$ in the unsaturated region, where

$$\begin{cases} \Delta e = -vT - \frac{1}{2}aT^2 \text{sat}(k_2[f(e) - v]), \\ \Delta v = aT \text{sat}(k_2[f(e) - v]). \end{cases}$$

Here it should be noted that the condition 6 was mistakenly formulated in [1] as "$|\dot{f}(e)| < \frac{1}{2T}$ for $\forall e$". The condition 7, as Workman pointed out in [1], is to guarantee the system state will remain in the unsaturated region, once in the unsaturated region. It was also shown that the trajectory of the closed-loop system starting from the saturated region will enter the unsaturated region in a finite time eventually.

Generally, as the velocity v is not measurable, an observer is needed to estimate the velocity. Further, there are always some disturbances in practical servo systems, which will cause steady-state error without proper compensation. Since the unknown disturbance is assumed to be piecewise constant or slowly varying and appear in the input channel (as an equivalent input disturbance), it can be modeled by a difference equation $d(k + 1) = d(k)$. Combining this equation with the plant model, we can obtain an augmented model, from which a reduced-order extended state observer can be designed to estimate the un-measured velocity and unknown disturbance. Choosing a conjugate pair of poles with the damping ratio ζ_0 and natural frequency ω_0 for the observer, the corresponding characteristic equation is $z^2 + q_1 z + q_0 = 0$, with

$$q_1 = -2e^{-\zeta_0\omega_0 T}\cos(\omega_0 T\sqrt{1 - \zeta_0^2}), \quad q_0 = e^{-2\zeta_0\omega_0 T}.$$

The dynamic equation of the observer is then given by

$$\begin{cases} x_v(k + 1) = A_v \cdot x_v(k) + B_u \cdot \text{sat}(u(k)) + B_y \cdot y(k), \\ \begin{pmatrix} \hat{v}(k) \\ \hat{d}(k) \end{pmatrix} = x_v(k) + L_y \cdot y(k) \end{cases} \quad (8)$$

where

$$\begin{cases} A_v = \begin{bmatrix} \frac{q_0 - q_1 - 1}{2} & \frac{aT}{4}(1 + q_0 - q_1) \\ -\frac{1 + q_0 + q_1}{aT} & \frac{1 - q_0 - q_1}{2} \end{bmatrix}, \\ B_u = \begin{bmatrix} \frac{aT}{4}(1 + q_0 - q_1) \\ -\frac{1 + q_0 + q_1}{2} \end{bmatrix}, \\ B_y = \begin{bmatrix} -\frac{4 - 4q_0 + 3q_1 - q_0 q_1 + q_1^2}{2T} \\ -\frac{2 + 2q_0 + 3q_1 + q_0 q_1 + q_1^2}{aT^2} \end{bmatrix}, \\ L_y = \begin{bmatrix} \frac{q_1 - q_0 + 3}{2T} \\ \frac{1 + q_0 + q_1}{aT^2} \end{bmatrix}. \end{cases}$$

Based on the above observer, a discrete-time PTOS control law with disturbance compensation is given as follows,

$$u_P(k) = \text{sat}\left(k_2[f(e(k)) - \hat{v}(k)] - \hat{d}(k)\right). \quad (9)$$

Next, let

$$\tilde{v}(k) = \hat{v}(k) - v(k), \quad \tilde{d}(k) = \hat{d}(k) - d, \quad w(k) = \begin{pmatrix} \tilde{v}(k) \\ \tilde{d}(k). \end{pmatrix}$$

It is easy to verify that

$$w(k + 1) = A_v \cdot w(k).$$

Choose a positive definite symmetric matrix $Q_v \in \mathbb{R}^{2 \times 2}$, and solve the following Lyapunov equation

$$P_v = A_v^T P_v A_v + Q_v, \quad (10)$$

for a matrix $P_v > 0$. Such a P_v always exists as A_v is asymptotically stable.

The PTOS control law (9) can be rewritten as

$$u_P(k) = \text{sat}(k_2[f(e(k)) - v(k)] - k_2 K_v \cdot w(k) - d)$$

with $K_v = \begin{bmatrix} 1 & \frac{1}{k_2} \end{bmatrix}$.

Then, the closed-loop system comprising (3) and (9) can be rewritten as

$$\begin{cases} e(k + 1) = e(k) - v(k)T - \frac{1}{2}aT^2(u_P(k) + d), \\ v(k + 1) = v(k) + aT(u_P(k) + d), \\ w(k + 1) = A_v \cdot w(k), \\ u_P(k) = \text{sat}(k_2[f(e(k)) - v(k) - K_v \cdot w(k)] - d). \end{cases} \quad (11)$$

Note that from the state feedback PTOS control (4) to the observer-based PTOS control (11), there are two additional terms of $w(k)$ and d in the latter case, while $w(k)$ converges to zero gradually. Similar to the state feedback case presented in [1], any trajectory of the closed-loop system (11) starting from the saturated region will enter the unsaturated region in a finite time eventually and will remain in the unsaturated region, once in the unsaturated region provided that the condition 7 is replaced by the following conditions:

7A. $|k_2[f(e + \Delta e) - (v + \Delta v) - K_v A_v w] - d| < u_{\max}$ for $\forall(e, v, w)$ in the unsaturated region, where $\Delta e = -vT - \frac{1}{2}aT^2(u_P + d)$, $\Delta v = aT(u_P + d)$.

7B. The unknown disturbance is bounded, i.e., $|d| \leqslant \delta u_{\max}$ for some positive parameter $\delta \in (0, 1)$.

7C. The initial estimation error $w(0)$ belongs to a two-dimensional set defined as

$$\Omega := \{w \in \mathbb{R}^2 : w^T P_v w < \lambda_\delta\},$$

where $\lambda_\delta > 0$ is the largest positive value such that

$$w(k) \in \Omega \Rightarrow |[k_2 \quad 1]w(k)| \leqslant (1 - \delta)u_{\max}. \quad (12)$$

The meaning of the condition 7A is the same as that of the condition 7 in the state feedback case. Conditions 7B and 7C ensure that the existence of disturbance and estimation error does not change the direction of acceleration when the control is saturated. Following the similar lines of reasoning as in [1], we can show that, the closed-loop system (11) is stable when the control input is saturated. For the case that the control input signal does not exceed the saturation level, the closed-loop system (11) can be written as follows,

$$\begin{cases} e(k + 1) = e(k) - v(k)T - \frac{mT}{2}[f(e(k)) - v(k) - K_v \cdot w(k)], \\ v(k + 1) = v(k) + m[f(e(k)) - v(k) - K_v \cdot w(k)], \\ w(k + 1) = A_v \cdot w(k). \end{cases} \quad (13)$$

where $m = aTk_2$.

To prove that the closed-loop system (13) is asymptotically stable, the following Lyapunov function is defined,

$$V_P(k) = p_v v^2(k) + \int_0^{e(k)} f(\sigma)d\sigma + w^T(k)P_v w(k), \quad (14)$$

where p_v is a positive scalar to be selected later. The increment of the Lyapunov function (14) along the trajectory of the closed-loop system (13) is given by

$$\Delta V_P(k) = V_P(k+1) - V_P(k)$$

$$= p_v[v^2(k+1) - v^2(k)] + \int_{e(k)}^{e(k+1)} f(\sigma)d\sigma + w^T(k+1)P_v w$$

$$\times (k+1) - w^T(k)P_v w(k) \tag{15}$$

Note that the integration term can be expressed using the Taylor expansion as follows,

$$\int_{e(k)}^{e(k+1)} f(\sigma)d\sigma = f(e(k))[e(k+1) - e(k)]$$

$$+ \frac{1}{2}\dot{f}(\xi)[e(k+1) - e(k)]^2$$

$$\leqslant f(e(k))[e(k+1) - e(k)]$$

$$+ c[e(k+1) - e(k)]^2. \tag{16}$$

for ξ between $e(k)$ and $e(k+1)$ ($k = 0, 1, 2, \ldots$), and

$$c := \sup|\frac{1}{2}\dot{f}(\xi)|,$$

Hence,

$$\Delta V_P(k) \leqslant p_v[v^2(k+1) - v^2(k)] - w^T(k)Q_v w(k) + f(e(k))[e(k+1) - e(k)] + c[e(k+1) - e(k)]^2, \tag{17}$$

Note that

$$v^2(k+1) - v^2(k) = (m^2 - 2m)v^2(k) + m^2 f^2(e(k)) + (2m - 2m^2)v(k)f(e(k)) + m^2 w^T(k)K_v^T K_v w(k) - 2m^2 K_v w(k)f(e(k)) + (2m^2 - 2m)K_v w(k)v(k),$$

and

$$e(k+1) - e(k) = -\frac{mT}{2}f(e(k)) + \left(\frac{m}{2} - 1\right)Tv(k) + \frac{mT}{2}K_v w(k),$$

Thus,

$$\Delta V_P(k) \leqslant \left[p_v(m^2 - 2m) + c\left(1 - \frac{m}{2}\right)^2 T^2\right]v^2(k) + \left[p_v m^2 - \frac{mT}{2} + \frac{1}{4}cm^2 T^2\right]f^2(e(k)) + \left[p_v(2m - 2m^2) + \left(\frac{m}{2} - 1\right)T\right]v(k)f(e(k))$$

$$+ c\left(m - \frac{m^2}{2}\right)T^2 v(k)f(e(k)) + w^T(k)\left[\left(p_v m^2 + \frac{1}{4}cm^2 T^2\right)K_v^T K_v - Q_v\right]w(k) + \left(-2p_v m^2 + \frac{mT}{2} - \frac{1}{2}cm^2 T^2\right)K_v w(k)f(e(k))$$

$$+ \left[p_v(2m^2 - 2m) + c\left(\frac{1}{2}m^2 - m\right)T^2\right]K_v w(k)v(k) = \begin{pmatrix} v(k) \\ w(k) \end{pmatrix}^T P \begin{pmatrix} v(k) \\ w(k) \end{pmatrix} + \begin{pmatrix} v(k) \\ w(k) \end{pmatrix}^T M f(e(k)) + N f^2(e(k)), \tag{18}$$

where

$$P = P^T = \begin{bmatrix} p_{11} & p_{12} \\ p_{12}^T & p_{22} \end{bmatrix}, \quad M = \begin{bmatrix} m_1 \\ m_2 \end{bmatrix},$$

with

$$\begin{cases} p_{11} = p_v(m^2 - 2m) + c(1 - \frac{m}{2})^2 T^2, \\ p_{12} = \frac{1}{2}\left[p_v(2m^2 - 2m) + c(\frac{1}{2}m^2 - m)T^2\right]K_v, \\ p_{22} = \left(p_v m^2 + \frac{1}{4}cm^2 T^2\right)K_v^T K_v - Q_v, \\ m_1 = p_v(2m - 2m^2) + (\frac{m}{2} - 1)T + c(m - \frac{1}{2}m^2)T^2, \\ m_2 = \left(-2p_v m^2 + \frac{1}{2}mT - \frac{1}{2}cm^2 T^2\right)K_v^T, \end{cases} \tag{19}$$

and

$$N = p_v m^2 - \frac{1}{2}mT + \frac{1}{4}cm^2 T^2.$$

Obviously, to ensure the right-hand side of (18) is negative definite, the following conditions must be satisfied:

$$\begin{cases} P < 0, \\ N - \frac{1}{4}M^T P^{-1}M \leqslant 0. \end{cases} \tag{20}$$

First, to ensure $P < 0$, we need

$$p_{11} < 0 \quad \text{and} \quad p_{22} - p_{12}^T p_{11}^{-1} p_{12} < 0,$$

The first inequality implies that,

$$0 < m < 2 \quad \text{and} \quad p_v > \frac{cT^2(2 - m)}{4m}. \tag{21}$$

The second inequality is satisfied if Q_v is chosen as follows,

$$Q_v > \left(p_v m^2 + \frac{1}{4}cm^2 T^2\right)K_v^T K_v - p_{12}^T p_{11}^{-1} p_{12}. \tag{22}$$

To ensure $N - \frac{1}{4}M^T P^{-1}M \leqslant 0$, it requires that

$$N \leqslant 0 \quad \text{and} \quad 4Np_{11} - m_1^2 \geqslant S(\bar{p}_{12}m_1 - p_{11}\bar{m}_2)^2, \tag{23}$$

with

$$\begin{cases} S = K_v(p_{11}p_{22} - p_{12}^T p_{12})^{-1}K_v^T, \\ \bar{p}_{12} = \frac{1}{2}\left[p_v(2m^2 - 2m) + c(\frac{1}{2}m^2 - m)T^2\right], \\ \bar{m}_2 = -2p_v m^2 + \frac{1}{2}mT - \frac{1}{2}cm^2 T^2. \end{cases} \tag{24}$$

Note that

$$\begin{cases} 4Np_{11} - m_1^2 = -(2p_v m - T + \frac{1}{2}mT)^2, \\ \bar{p}_{12}m_1 - p_{11}\bar{m}_2 = -p_v m(2p_v m - T + \frac{1}{2}mT), \end{cases}$$

and $S > 0$, thus the second inequality in (23) leads to

$$(Sp_v^2 m^2 + 1)\left(2p_v m - T + \frac{1}{2}mT\right)^2 \leqslant 0, \tag{25}$$

which implies that

$$2p_v m - T + \frac{1}{2}mT = 0, \tag{26}$$

or

$$p_v = \frac{T(2 - m)}{4m}. \tag{27}$$

The inequality $N \leqslant 0$ is equivalent to

$$p_v \leqslant \frac{T(2 - cTm)}{4m}. \tag{28}$$

Combining the above results with (21), we can obtain

$$0 < cT < 1. \tag{29}$$

Note that (21) and (29) are actually guaranteed by the condition 1 and 6 respectively. Hence, it is obvious that the appropriate $p_v > 0$ and $Q_v > 0$ always exist such that,

$$\Delta V_{\mathrm{P}}(k) \leqslant 0. \tag{30}$$

As in its continuous-time counterpart, it is then straightforward to verify the closed-loop system comprising the PTOS control law with measurement feedback and the given plant is asymptotically stable.

2.2. Discrete-time observer-based CNF control

In this subsection, we proceed to design a discrete-time CNF control law for the plant (1), which eventually will be employed in our MSC framework.

First we note that the same observer in (8) is adopted here. Following the procedure in [9], a CNF control law with disturbance compensation is designed as

$$u_{\mathrm{c}}(k) = F\binom{y(k)}{\hat{v}(k)} + Gr + \rho(e(k))F_n\binom{y(k) - r}{\hat{v}(k)} - \hat{d}(k), \tag{31}$$

where $F = [f_1 \ \ f_2]$ is the linear feedback gain matrix such that the eigenvalues of $A + BF$ are on the desired locations. The feed-forward gain for target reference can be determined as $G = -f_1$. The nonlinear feedback gain matrix $F_n = [f_{n1} \ \ f_{n2}]$ is given by

$$F_{\mathrm{n}} = B^T P_{\mathrm{x}}(A + BF), \tag{32}$$

where $P_{\mathrm{x}} > 0$ is the solution to the following Lyapunov equation

$$P_{\mathrm{x}} = (A + BF)^T P_{\mathrm{x}}(A + BF) + W_{\mathrm{x}}, \tag{33}$$

for any chosen symmetric positive definite matrix $W_{\mathrm{x}} \in \mathbb{R}^{2 \times 2}$. Such a P_{x} always exists as $A + BF$ is asymptotically stable. The gain function $\rho(e(k))$ is a smooth and non-positive function of $|e(k)|$, and is used to tune the control laws so as to improve the performance of closed-loop system as the controlled output $y(k)$ approaches the target reference r.

Define

$$x_{\mathrm{e}} = \binom{r}{0}, \quad \tilde{x}(k) = x(k) - x_{\mathrm{e}}. $$

Note that the CNF control law in (31) can be rewritten as,

$$u_{\mathrm{c}}(k) = ([F \ \ F_{\mathrm{v}}] + \rho(e(k))[F_n \ \ F_{n\mathrm{v}}])\binom{\tilde{x}(k)}{w(k)} - d, \tag{34}$$

with $F_{\mathrm{v}} = [f_2 \ \ -1], F_{n\mathrm{v}} = [f_{n2} \ \ 0], w(k) = \binom{\tilde{v}(k)}{\tilde{d}(k)}$.

Next, choose the symmetric positive definite matrix $Q_{\mathrm{v}} \in \mathbb{R}^{2 \times 2}$ to satisfy (22) and the following condition:

$$Q_{\mathrm{v}} > F_{\mathrm{v}} B^T [P_{\mathrm{x}} + P_{\mathrm{x}}(A + BF)W_{\mathrm{x}}^{-1}(A + BF)^T P_{\mathrm{x}}]BF_{\mathrm{v}}^T \tag{35}$$

and solve the Lyapunov equation in (10) for a matrix P_{v}.

Now, assuming the disturbance is bounded by $\delta u_{\max}$ for some positive variable $\delta \in (0, 1)$, we define a set

$$\mathbf{X} := \left\{ \binom{\tilde{x}}{w} \in \mathbb{R}^4 : \binom{\tilde{x}}{w}^T \begin{bmatrix} P_{\mathrm{x}} & 0 \\ 0 & P_{\mathrm{v}} \end{bmatrix} \binom{\tilde{x}}{w} \leqslant c_\delta \right\}, \tag{36}$$

where $c_\delta > 0$ is the largest positive value such that

$$\binom{\tilde{x}}{w} \in \mathbf{X} \Rightarrow \left| [F \ \ F_{\mathrm{v}}]\binom{\tilde{x}}{w} \right| \leqslant (1 - \delta)u_{\max}. \tag{37}$$

The error dynamics equation of the plant in (1) can be expressed as,

$$\tilde{x}(k+1) = x(k+1) - x_{\mathrm{e}} = (A + BF)\tilde{x}(k) + BF_{\mathrm{v}}w(k) + B s(k), \tag{38}$$

where

$$s(k) := \mathrm{sat}(u_{\mathrm{c}}(k)) - [F \ \ F_{\mathrm{v}}]\binom{\tilde{x}(k)}{w(k)} + d. \tag{39}$$

For simplicity of presentation, we will omit the time index (k) in the following derivation so long as no confusion is caused. We may also omit the variable $e(k)$ of nonlinear function $\rho(e(k))$ as appropriate. Now, for the disturbance bounded by $\delta u_{\max}$ and $\binom{\tilde{x}(k)}{w(k)} \in \mathbf{X}$,

$$\left| [F \ \ F_{\mathrm{v}}]\binom{\tilde{x}(k)}{w(k)} - d \right| \leqslant u_{\max}, $$

hence the value of $s(k)$ can be written in three cases according to the range of control u_c,

$$\begin{cases} \rho[F_n \ \ F_{n\mathrm{v}}]\binom{\tilde{x}}{w} < s < 0, & u_c < -u_{\max}, \\ s = \rho[F_n \ \ F_{n\mathrm{v}}]\binom{\tilde{x}}{w}, & |u_c| \leqslant u_{\max}, \\ 0 < s < \rho[F_n \ \ F_{n\mathrm{v}}]\binom{\tilde{x}}{w}, & u_c > u_{\max}. \end{cases} \tag{40}$$

Obviously, for all possible situations, we can always write s as

$$s = q\rho[F_n \ \ F_{n\mathrm{v}}]\binom{\tilde{x}}{w}, \tag{41}$$

for some non-negative variable $q \in [0, 1]$. Thus, for the case when $\binom{\tilde{x}}{w} \in \mathbf{X}$, the closed-loop system comprising the given plant (1) and the control law (8) and (31) can be expressed as follows,

$$\binom{\tilde{x}(k+1)}{w(k+1)} = \begin{bmatrix} A + BF + q\rho BF_n & A_\rho \\ 0 & A_\mathrm{v} \end{bmatrix} \binom{\tilde{x}(k)}{w(k)}, \tag{42}$$

where

$$A_\rho = BF_\mathrm{v} + q\rho BF_{n\mathrm{v}}. $$

Define a Lyapunov function

$$V_{\mathrm{C}}(k) = \binom{\tilde{x}(k)}{w(k)}^T \begin{bmatrix} P_{\mathrm{x}} & 0 \\ 0 & P_{\mathrm{v}} \end{bmatrix} \binom{\tilde{x}(k)}{w(k)}, \tag{43}$$

and evaluate its increment along the trajectories of the closed-loop system (42),

$$\begin{aligned} \Delta V_{\mathrm{C}}(k) &= V_{\mathrm{C}}(k+1) - V_{\mathrm{C}}(k) \\ &= -\tilde{x}^T(k)W_{\mathrm{x}}\tilde{x}(k) + \tilde{x}(k)^T F_n^T (2q\rho + q^2\rho^2 B^T P_{\mathrm{x}}B)F_n\tilde{x}(k) \\ &\quad + 2\tilde{x}^T(k)(A + BF)^T(P_{\mathrm{x}} + q\rho P_{\mathrm{x}}BB^T P_{\mathrm{x}})A_\rho w(k) \\ &\quad + w^T(k)A_\rho^T P_{\mathrm{x}}A_\rho w(k) - w^T(k)Q_\mathrm{v}w(k). \end{aligned}$$

If the nonlinear gain function ρ is chosen such that $\rho \in [-2(B^T P_{\mathrm{x}}B)^{-1}, 0]$, then

$$2q\rho + q^2\rho^2 B^T P_{\mathrm{x}}B \leqslant 0. $$

Hence, we have

$$\begin{aligned} \Delta V_{\mathrm{C}}(k) &\leqslant -\tilde{x}(k)^T W_{\mathrm{x}}\tilde{x}(k) + 2\tilde{x}^T(k)(A + BF)^T P_\rho A_\rho w(k) - w^T(k)(Q_\mathrm{v} \\ &\quad - A_\rho^T P_{\mathrm{x}}A_\rho)w(k) = -\binom{\tilde{x}_w(k)}{w(k)}^T \begin{bmatrix} W_{\mathrm{x}} & 0 \\ 0 & Q_{\mathrm{s}} \end{bmatrix} \binom{\tilde{x}_w(k)}{w(k)}. \end{aligned}$$

where

$$P_\rho = P_x + q\rho P_x BB^T P_x,$$
$$\tilde{x}_w(k) = \tilde{x}(k) - W_x^{-1}(A + BF)^T P_\rho A_\rho w(k),$$
$$Q_s = Q_v - A_\rho^T[P_x + P_\rho(A + BF)W_x^{-1}(A + BF)^T P_\rho]A_\rho.$$

By the choice of Q_v in (35), there exists a scalar $\hat{\rho} > 0$ such that for any smooth and non-positive function $\rho(e(k))$ with $|\rho(e(k))| \leqslant \hat{\rho}$, we have $Q_s > 0$. Clearly, the closed-loop system with those assumptions, has $\Delta V_C(k) \leqslant 0$ and thus is asymptotically stable. Hence, we conclude that $x(k) \to x_e$ as $k \to \infty$, and the output $y(k)$ asymptotically tracks the target reference r. Obviously, **X** is an invariant set of the closed-loop system comprising the reduced-order CNF controller. The trajectory of the closed-loop system will remain in **X** and converge to the origin, once it enters into **X**.

2.3. Discrete-time MSC control scheme

In this subsection, a discrete-time MSC control scheme which combines the PTOS and CNF control laws with reduced-order observer for the plant (1) is presented, which takes the form as follows,

$$u(k) = \begin{cases} u_P(k), & k < k_s, \\ u_C(k), & k \geqslant k_s, \end{cases} \quad (44)$$

where k_s is the time index that the MSC control switches from PTOS to CNF, and is determined by the mode switching conditions given by

$$\begin{pmatrix} \tilde{x}(k_s) \\ w(k_s) \end{pmatrix} \in \mathbf{X} \text{ and } |e(k_s)| \leqslant y_l, \quad (45)$$

where y_l is the size of the linear region of the PTOS control law. The PTOS control law $u_P(k)$ and the CNF control law $u_c(k)$ are as follows,

$$\begin{cases} u_P(k) = \text{sat}\{k_2[f(e(k)) - \hat{v}(k)] - \hat{d}(k)\}, \\ u_c(k) = [F + \rho(e(k))F_n]\begin{pmatrix} y(k) - r \\ \hat{v}(k) \end{pmatrix} - \hat{d}(k), \end{cases} \quad (46)$$

where r is the target reference and $e(k) = r - y(k)$ is the tracking error. $\hat{v}(k)$ and $\hat{d}(k)$ are the output of the observer in (8), which is shared by the PTOS control law with the CNF control law. The CNF nonlinear function $\rho(e(k))$ is chosen as

$$\rho(e(k)) = -\beta \times \arctan\left(\lambda \times \left\|\frac{e(k)}{e(k_s)}\right\| - \lambda_s\right) \quad (47)$$

with $0 \leqslant \beta \leqslant \frac{4}{\pi}(B^T P_x B)^{-1}$. The parameter $\lambda > 0$ is used to determine the speed of change in $\rho(e(k))$, and $e(k_s)$ represents the tracking error upon mode switching. The value of λ_s can be chosen to ensure that the magnitude of $\rho(e(k))$ is increscent as $|e(k)|$ tends to zero and that there is no jerk in the control signal during mode switching, i.e.,

$$\lambda_s = 1 + \frac{1}{\lambda} \tan\left(\left\|\frac{([k_1 \quad k_2] + F)\hat{\tilde{x}}(k_s)}{\beta F_n \hat{\tilde{x}}(k_s)}\right\|\right), \quad (48)$$

where $\hat{\tilde{x}}(k_s) = \begin{pmatrix} y(k_s) - r \\ \hat{v}(k_s) \end{pmatrix}$.

Next, we proceed to analyze the stability of the closed-loop system comprising the discrete-time MSC control law (44) and the plant (1). For the case that the control input is saturated, where only the PTOS control is effective, it has been proved that the closed-loop system is stable, and any trajectory starting from the saturated region will enter the unsaturated region in finite time eventually and the trajectory will remain in the unsaturated

region, once in the unsaturated region. Hence, we only need to analyze the stability in the unsaturated region for the closed-loop system with the MSC control law (44).

We re-express (14) using the Taylor expansion as follows:

$$V_P(k) = p_v v^2(k) + \frac{1}{2}\dot{f}(\tau)e^2(k) + w^T(k)P_v w(k) = \begin{pmatrix} \tilde{x}(k) \\ w(k) \end{pmatrix}^T \begin{bmatrix} \frac{1}{2}\dot{f}(\tau) & 0 & 0 \\ 0 & p_v & 0 \\ 0 & 0 & P_v \end{bmatrix} \begin{pmatrix} \tilde{x}(k) \\ w(k) \end{pmatrix}, \quad (49)$$

where τ is an appropriate scalar between 0 and $e(k)$. Let

$$\gamma = \min\left\{\frac{1}{2}\dot{f}(\tau), p_v, \lambda_{\min}(P_v)\right\} / \max\{\lambda_{\max}(P_x), \lambda_{\max}(P_v)\}. \quad (50)$$

The Lyapunov function for the overall closed-loop system with the MSC control law (44) can be chosen as

$$V(k) = V_P(k)[1 - 1(k - k_s)] + \gamma V_C(k) \cdot 1(k - k_s), \quad (51)$$

where

$$1(k - k_s) = \begin{cases} 0, & k < k_s, \\ 1, & k \geqslant k_s. \end{cases}$$

It is simple to verify that

$$\Delta V(k) = \Delta V_P(k)[1 - 1(k + 1 - k_s)] + \gamma \Delta V_C(k) \cdot 1(k + 1 - k_s)$$
$$+ (\gamma V_C(k) - V_P(k))[1(k + 1 - k_s) - 1(k - k_s)].$$

It has already been proved that the increment of the Lyapunov function $V_P(k)$ and $V_C(k)$ are negative definite when they are effective respectively. The last item is always non-positive in view of the definition of γ in (50). Hence, $\Delta V(k) \leqslant 0$ and the resulting closed-loop system comprising the given plant and the MSC control law is asymptotically stable. Furthermore, (45) gives the mode switching condition for the proposed MSC scheme.

There are some guidelines for choosing the controller parameters. For the PTOS control law, the natural frequency ω is consistent with the desired closed-loop servo bandwidth. The acceleration discount factor α takes value between 0 and 1, and normally the largest possible value is desired. But, to allow for the plant uncertainty, a sensible range for α is [0.9, 0.95]. The damping ratio ζ is chosen such that the overshoot is kept within the specified level. Specifically, if the PTOS control law is implemented as an independent controller, ζ should be no smaller than 0.8 to ensure an overshoot below 2%. For the MSC control scheme, since the settling process will be taken over by CNF, the PTOS damping ratio ζ can be reduced to around 0.7 for faster targeting. The initial damping ratio of CNF should be small (typically 0.3), and the natural frequency should also be consistent with the desired servo bandwidth. The matrix W_x can be chosen to be diagonal, while the parameters $\beta \in \left[0, \frac{4}{\pi}(B^T P_x B)^{-1}\right]$ and $\lambda > 0$ can be determined from the root locus by choosing the desired steady-state locations of closed-loop poles (see [9] for more details) or by some tuning methods (see e.g., [10]). For the parameter c_δ of the CNF invariant set, an estimation which might be conservative, is given by Ref. [19]

$$c_\delta = \frac{[(1 - \delta)u_{\max}]^2}{\bar{F}\bar{P}_x^{-1}\bar{F}^T}. \quad (52)$$

with $\bar{F} = [F \quad F_v]$ and $\bar{P}_x = \begin{bmatrix} P_x & 0 \\ 0 & P_v \end{bmatrix}$. Finally, for the extended state observer, the natural frequency ω_0 of its poles should be no smaller than three times the desired closed-loop bandwidth, and damping ratio ζ_0 can be simply fixed as $\frac{\sqrt{2}}{2}$ (Butterworth pattern).

3. Application in PMSM position regulation

In this section we apply the discrete-time MSC control scheme to design a position controller for permanent magnet synchronous motor servo systems. PMSM has found extensive applications in high speed and precision servo systems (see e.g., [14–18]), due to the advantages of light weight, high efficiency and compact structure. In this paper, we deal with the surface-mounted PMSMs, with the dq model given by

$$\begin{cases} u_q = R_s i_q + L_q \frac{di_q}{dt} + n_p \omega_r L_d i_d + n_p \omega_r \psi_f \\ u_d = R_s i_d + L_d \frac{di_d}{dt} - n_p \omega_r L_q i_q \\ T_e = 1.5 n_p \psi_f i_q = J \frac{d\omega_r}{dt} + k_b \omega_r + T_L \\ \frac{d\theta_r}{dt} = \omega_r \end{cases}$$

where u_d and u_q are the input voltages in dq frame, i_d and i_q are the electric currents, L_d and L_q are the inductances, R_s is the stator resistance, n_p is the number of pole pairs, ψ_f is the flux linkage established by permanent magnet, ω_r and θ_r are the mechanical angular speed and angle, T_e is the electromagnetic torque, T_L is the load torque, J is the moment of inertia of motor, k_b is the viscous friction coefficient.

In conventional PMSM servo systems, the cascaded structure of position–speed–current loops is adopted, with PID as the dominant control method. In our study, the electric current loops are still controlled by PID, but the position and speed loops have been unified and controlled by the MSC control law. Taking the angular position θ_r (rad) of motor as the system output y, and i_q as the control signal u (to be used as the target reference for the i_q control loop), we obtain a double integrator plant, as characterized by (1), with the parameter $a = \frac{1.5 n_p \psi_f}{J}$.

The PMSM in our study is of model 60CB020C, with 3000RPM as the rated speed of rotation, and a rated torque of 0.6 Nm, the number of pole pairs is 4. It has an optical encoder of 2500 counts per revolution for position measurement. The amplitude of the electric current i_q is limited by 1.5 A, i.e., $u_{max} = 1.5$ A. The value of system parameter has been identified as $a = 1120$, and a sampling period of $T = 0.002$ s is chosen for digital control of PMSM position servo system.

Following the design procedure of MSC, we first choose the damping ratio, natural frequency, and the acceleration discount factor of the PTOS control law as follows,

$$\zeta = 0.68, \quad \omega = 35, \quad \alpha = 0.9,$$

then the feedback gains and relevant parameters of PTOS are computed as,

$$k_1 = 1.0429, \quad k_2 = 0.0416, \quad J_0 = 30.144, \quad y_l = 1.2019.$$

Now the PTOS control law can be given by

$$u_P(k) = \text{sat}\left(k_2[f(e(k)) - \hat{v}(k)] - \hat{d}(k) \right), \tag{53}$$

where $e(k) = r - y(k)$, and $f(e(k))$ is as given in (5).

The estimated velocity $\hat{v}(k)$ and disturbance $\hat{d}(k)$ are provided by the observer for which the conjugate poles are chosen to have a damping ratio 0.707 and a natural frequency 110. The dynamic equation of the observer is given by

$$\begin{cases} x_v(k+1) = \begin{bmatrix} 0.7119 & 1.9174 \\ -0.0185 & 0.9793 \end{bmatrix} \cdot x_v(k) \\ \qquad + \begin{bmatrix} 1.9174 & -23.758 \\ -0.0207 & -2.8553 \end{bmatrix} \cdot \begin{pmatrix} \text{sat}(u(k)) \\ y(k) \end{pmatrix}, \\ \begin{pmatrix} \hat{v}(k) \\ \hat{d}(k) \end{pmatrix} = x_v(k) + \begin{bmatrix} 144.03 \\ 9.2474 \end{bmatrix} \cdot y(k) \end{cases} \tag{54}$$

Next, to design the CNF control law, we choose a damping ratio 0.3 and a natural frequency 35 for the pair of closed-loop poles, and obtain the linear feedback gain matrix as

$$F = -[1.0707 \quad 0.0194].$$

We choose a positive definite matrix $W_x = \text{diag}(0.002, 0.002)$ and solve the Lyapunov equation in (33) to obtain

$$P_x = \begin{bmatrix} 29.224 & 1.0208 \times 10^{-3} \\ 1.0208 \times 10^{-3} & 2.4843 \times 10^{-2} \end{bmatrix}.$$

The CNF nonlinear feedback gain is computed as
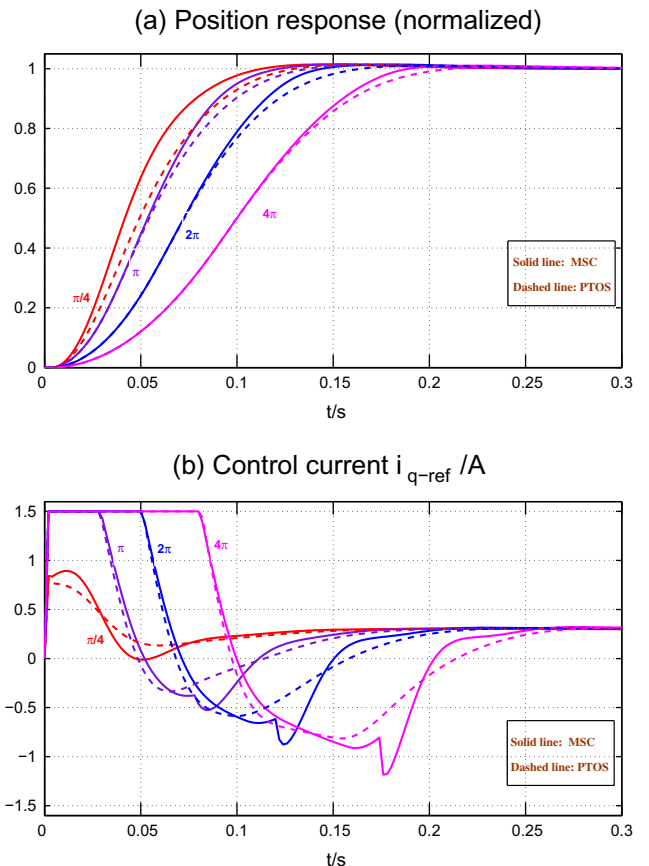
$$F_n = [-0.0659 \quad 0.0534].$$

Based on the observer in (54), the CNF control law is given by,

$$u_C(k) = [F + \rho(e(k))F_n]\begin{pmatrix} y(k) - r \\ \hat{v}(k) \end{pmatrix} - \hat{d}(k), \tag{55}$$

where $\rho(e(k))$ is as given in (47) with $\beta = 0.5$, $\lambda = |e(0)|$, and the parameter λ_s is computed according to (48) at the switching instant.
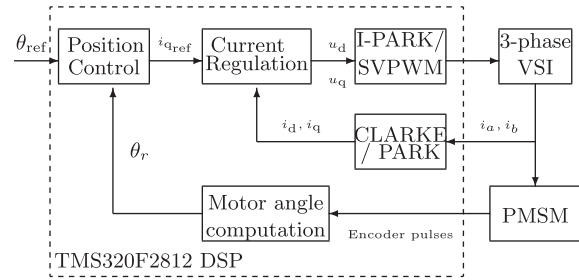
Table 1
PID parameters for current loops.

	k_p	k_i	k_d
i_q Loop	19.053	0.1905	18.1
i_d Loop	43.301	0.1443	0

(a) Position response (normalized)

Solid line: MSC
Dashed line: PTOS

(b) Control current i_{q-ref} /A

Solid line: MSC
Dashed line: PTOS

Fig. 2. Comparisons of simulation results between the MSC and PTOS control with a disturbance $d = -0.3$ A.

Table 2
Comparison of settling time (s) in simulation.

Target angle θ (rad)	$\frac{\pi}{4}$	π	2π	4π
PTOS	0.117	0.124	0.148	0.191
MSC	0.101	0.110	0.134	0.178
Improvement	13.7%	11.3%	9.5%	6.8%

(a) Position response (normalized)

(b) Control current i_{q-ref} **/A**

Fig. 3. Simulation results with MSC for target angle 2π with disturbance $d = -0.5$ A and perturbations in system parameter a.

Fig. 4. Experimental setup of PMSM servo system.

For the cases when the initial system state is within the CNF invariant set, the CNF control law will be effective from the beginning without the need for control switching, and the parameters of $\rho(e(k))$ are chosen as $\beta = 0.5, \lambda = 2.8$, and $\lambda_s = 1$.

Now, the MSC control law which combines PTOS and CNF is given by

$$u(k) = \begin{cases} u_P(k), & k < k_s, \\ u_C(k), & k \geqslant k_s, \end{cases} \qquad (56)$$

Fig. 5. Block diagram of PMSM position servo system.

with the time index k_s determined by the first instant that the system enters into the following region:

$$|e(k)| \leqslant y_l \text{ and } \begin{pmatrix} y(k) - r \\ \hat{v}(k) \end{pmatrix}^T P_x \begin{pmatrix} y(k) - r \\ \hat{v}(k) \end{pmatrix} \leqslant c_\delta = 41.38. \qquad (57)$$

For the two current control loops of i_d and i_q, digital PID control laws with anti-windup feedback are adopted, with the sampling frequency of 20 kHz for control implementation and PWM generation. The parameters of PID controllers are summarized in Table 1.

To verify the design, simulations have been carried out in MATLAB/Simulink, using the nominal double integrator as the plant model (ignoring the electric current loops). For comparison, we also test a PTOS controller with parameters $\zeta = 0.8$, $\omega = 35, \alpha = 0.95$ and the same observer in (54). Simulations were done for various target angles. The results are shown in Fig. 2, and the performances in terms of settling time (with 2% error bound) are summarized in Table 2. It is clear that the MSC controller achieves faster settling in all the tracking tasks. Note that for $\alpha = 0.95$, the PTOS controller is supposed to achieve almost optimal performance (Workman [1]). However, the MSC controller works even better. This is because the MSC utilizes the advantages of both PTOS and CNF and the mode switching is smooth. To check the robustness of the MSC scheme with respect to system perturbations, simulations were done to track the target angle 2π with a disturbance $d = -0.5$ A and variations in the system parameter a. The results in Fig. 3 indicate that in the face of plant perturbations of up to 25%, the MSC controller with nominal design parameters can maintain a satisfactory performance with an overshoot below 2%, and no steady-state error. Obviously, the MSC scheme has some degree of robustness against the plant uncertainty.

Next, real-time implementations were conducted using the experimental setup shown in Fig. 4. A TMS320F2812DSP board (from Texas Instruments) was adopted for motor control under the Space Vector PWM pattern, with the proposed MSC scheme for position control. The structure of the servo system is given in Fig. 5. Experimental data were collected via the Code Composer Studio software system and then processed in MATLAB. Experiments were first carried out for various target angles of motor under the load torque 0.12 Nm (equivalently 20% of rated torque, note that there is some other disturbance besides the load torque in the system), the results are shown in Figs. 6–9. In these figures, the waveforms for the angular position, speed, control signal (the reference for i_q loop) and the estimated disturbance are provided. It is interesting to note that for target angle $\frac{\pi}{4}$, the PTOS control leads to an overshoot of 6% and a sluggish settling. Table 3 summarizes the performance in terms of settling time (with a 2% error bound), which clearly indicates the MSC control out-performs the PTOS control, with the overshoot kept within 2% and no
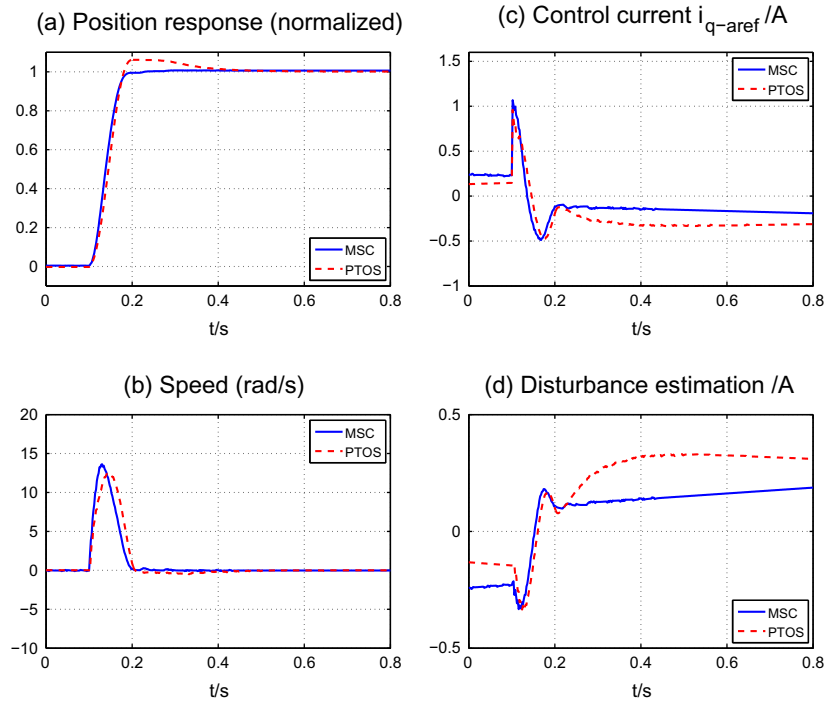
Fig. 6. Comparisons of experimental results between the MSC and PTOS control for target angle $\frac{\pi}{4}$.
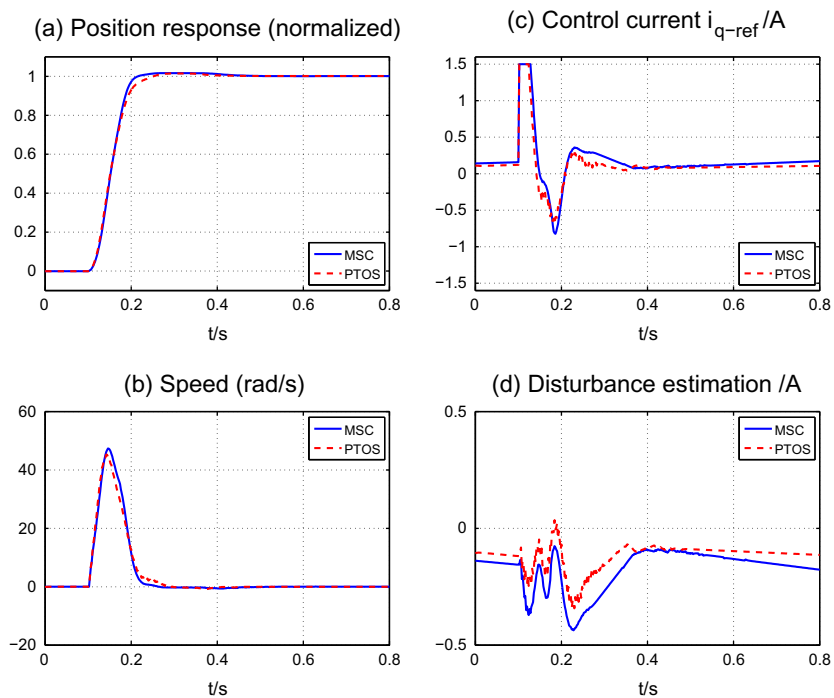

Fig. 7. Comparisons of experimental results between the MSC and PTOS control for target angle π.

steady-state error. Fig. 10 gives the results of the MSC control for the target angle π under various load torques (respectively 0%, 20%, 40% of rated torque). It is clear that the overall performance is still desirable and consistent in the face of unknown disturbance (among which is the load torque). With the proposed MSC control scheme, fast and smooth tracking can be achieved for a wide range of target references, with some robustness to the amplitude of load disturbance.
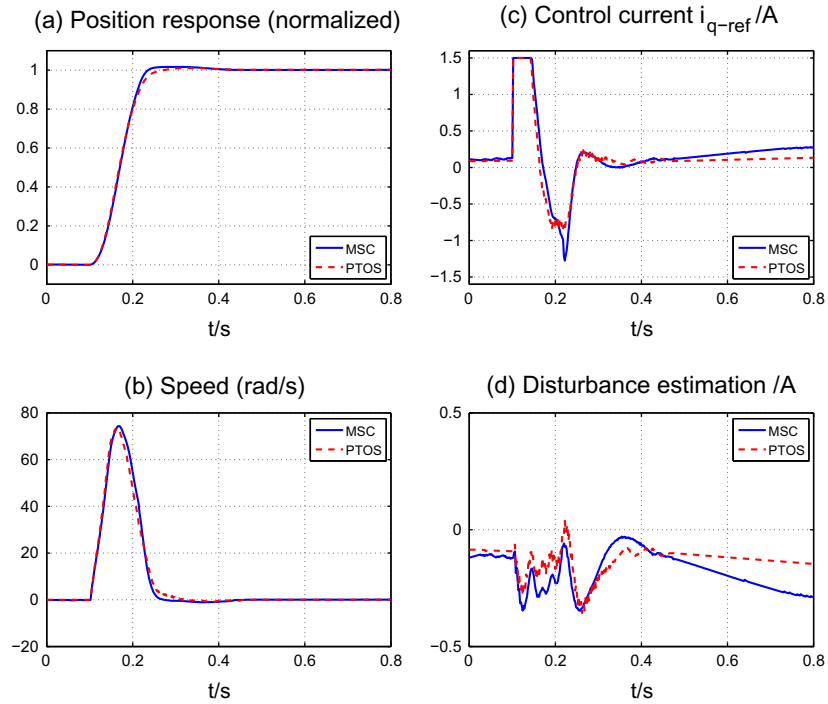
Fig. 8. Comparisons of experimental results between the MSC and PTOS control for target angle 2π.
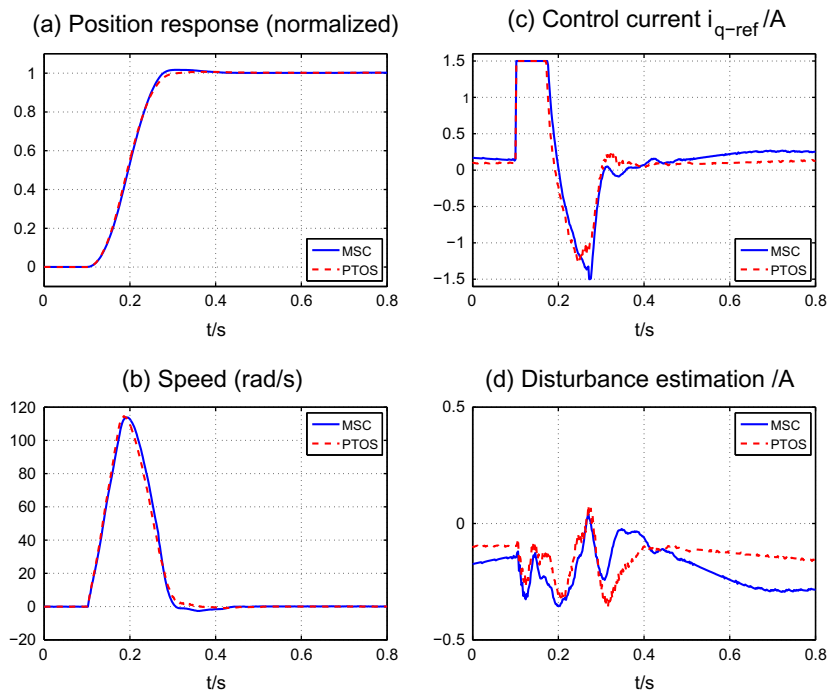

Fig. 9. Comparisons of experimental results between the MSC and PTOS control for target angle 4π.

Table 3
Comparison of settling time (s) in experiments.

Target angle θ (rad)	$\frac{\pi}{4}$	π	2π	4π
PTOS	0.272	0.128	0.142	0.180
MSC	0.082	0.102	0.128	0.170
Improvement	69.9%	20.3%	9.9%	5.6%

4. Concluding remarks

A discrete-time MSC control scheme has been proposed by combining the PTOS control and CNF control with an extended state observer. The closed-loop stability has been analyzed theoretically. The method has been adopted to design the position controller for a permanent magnet synchronous motor servo
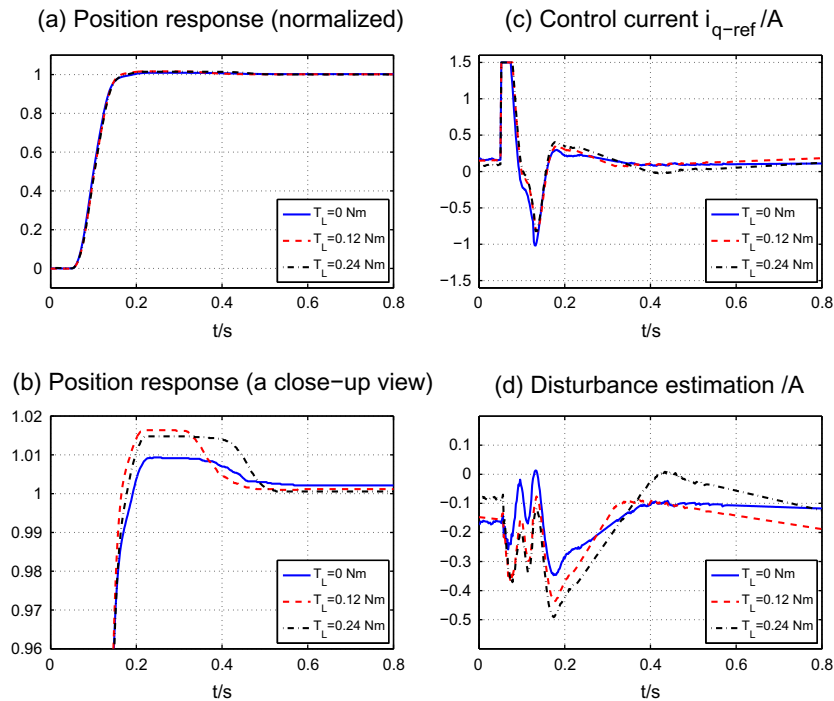
Fig. 10. Experimental results with MSC for target angle π under various load torques (a close-up view).

system. MATLAB simulation and experimental results based on TMS320F2812 show that the proposed MSC design is capable of tracking a wide range of target positions smoothly and accurately with a faster settling time. The proposed MSC control method can be easily applied to other servo systems with a double integrator model.

Acknowledgment

References

[1] Workman ML. Adaptive proximate time optimal servomechanisms. Ph.D. Dissertation, Stanford University; 1987.
[2] Dhanda A, Franklin GF. An improved 2-DOF proximate time optimal servomechanism. IEEE Trans Magn 2009;45(5):2151–64.
[3] Zhou J, Zhou R, Wang Y, et al. Improved proximate time optimal sliding-mode control of hard disk drives. IEE Proc Control Theory Appl 2001;11(6):516–22.
[4] Choi Y, Jeong J, Gweon D. A novel damping scheduling scheme for proximate time optimal servomechanisms in hard disk drives. IEEE Trans Magn 2006;42(3):468–72.
[5] Venkataramanan V, Chen BM, Lee TH, Guo G. A new approach to the design of mode switching control in hard disk drive servo systems. Control Eng Practice 2002;10:925–39.
[6] Lin Z, Pachter M, Banda S. Toward improvement of tracking performance – nonlinear feedback for linear system. Int J Control 1998;70(1):1–11.

[7] Chen BM, Lee TH, Peng K, Venkataramanan V. Composite nonlinear feedback control for linear systems with input saturation: theory and an application. IEEE Trans Autom Contr 2003;48(3):427–39.
[8] Peng K, Chen BM, Cheng G, Lee TH. Modeling and compensation of nonlinearities and friction in a micro hard disk drive servo system with nonlinear feedback control. IEEE Trans Contr Syst Technol 2005;13(5):708–21.
[9] Peng K, Cheng G, Chen BM, Lee TH. Improvement of transient performance in tracking control for discrete-time systems with input saturation and disturbances. IET Control Theory Appl 2007;1(1):65–74.
[10] Lan W, Thum CK, Chen BM. A hard disk drive servo system design using composite nonlinear feedback control with optimal nonlinear gain tuning methods. IEEE Trans Indust Electr 2010;57(5):1735–45.
[11] Peng K, Cai G, Chen BM, et al. Design and implementation of an autonomous flight control law for a UAV helicopter. Automatica 2009;45(10):2333–8.
[12] Cai G, Chen BM, Dong X, Lee TH. Design and implementation of a robust and nonlinear flight control system for an unmanned helicopter. Mechatronics 2011;21(5):803–20.
[13] Thum CK, Du C, Chen BM, et al. A unified control scheme for track seeking and following of a hard disk drive servo system. IEEE Trans Contr Syst Technol 2010;18(2):294–306.
[14] Tomei P, Verrelli CM. Observer-based speed tracking control for sensorless permanent magnet synchronous motors with unknown load torque. IEEE Trans Autom Contr 2011;56(6):1484–8.
[15] Choi HH, Jung JW. Takagi–Sugeno fuzzy speed controller design for a permanent magnet synchronous motor. Mechatronics 2011;21(8):1317–28.
[16] Corradini ML, Ippoliti G, Longhi S, Orlando G. A quasi-sliding mode approach for robust control and speed estimation of PM synchronous motors. IEEE Trans Indust Electr 2012;59(2):1096–104.
[17] Errouissi R, Ouhrouche M, Chen WH, Trzynadlowski AM. Robust cascaded nonlinear predictive control of a permanent magnet synchronous motor with antiwindup compensator. IEEE Trans Indust Electr 2012;59(8):3078–88.
[18] Vu NT, Choi HH, Jung JW. Certainty equivalence adaptive speed controller for permanent magnet synchronous motor. Mechatronics 2012;22(6):811–8.
[19] Khalil HK. Nonlinear systems. 3rd ed. Prentice Hall; 2002.